PAPER • **OPEN ACCESS**

Fine-tuning equilibrium water content and mechanical properties of acrylic-based copolymers for intraocular lens applications

To cite this article: Deniz Aki *et al* 2025 *Biomed. Mater.* **20** 045026

IOP Publishing Biomed. Mater. 20 (2025) 045026 https://doi.org/10.1088/1748-605X/ade8c7

Biomedical Materials

OPEN ACCESS

RECEIVED
26 October 2024

REVISED
15 June 2025

ACCEPTED FOR PUBLICATION
26 June 2025

PUBLISHED
9 July 2025

PAPER

Fine-tuning equilibrium water content and mechanical properties of acrylic-based copolymers for intraocular lens applications

Deniz Aki[1,2,3], **Monireh Esmaeili Rad**[3,4], **Esat Can Şenel**[3], **Mesut Celil Onceyiz**[3], **Melih Can Gokmenoglu**[3], **Liviu Duta**[5,*] and **Oguzhan Gunduz**[1,2,*]

[1] Center for Nanotechnology and Biomaterials Application & Research (NBUAM), Marmara University, Istanbul 34722, Turkey
[2] Faculty of Technology, Department of Metallurgical and Materials Engineering, Marmara University, Istanbul 34722, Turkey
[3] Research and Development Department, VSY Biotechnology, Istanbul 34959, Turkey
[4] Nanotechnology Research and Application Center (SUNUM), Sabanci University, Istanbul 34956, Turkey
[5] Lasers Department, National Institute for Laser, Plasma and Radiation Physics, 077125 Magurele, Romania
[*] Authors to whom any correspondence should be addressed.

E-mail: liviu.duta@inflpr.ro and ucemogu@ucl.ac.uk

Keywords: hydrophobic/hydrophilic monomer, acrylic-based copolymers, physical-chemical, optical, mechanical characterization, equilibrium water content, intraocular lens application

Abstract

We report on the development of copolymers of 2-hydroxy ethyl acrylate (HEA) with 2-(2-ethoxy ethoxy) ethyl acrylate (EEEA) grafted with ethylene glycol di-methacrylate, designed for use as an intraocular lens (IOL) material. Various HEA/EEEA monomer ratios were synthesized via thermal copolymerization, with the HEA concentration progressively increasing from 3.5% to 28%, while the EEEA concentration decreased proportionately. The physical-chemical, optical, and mechanical properties of the newly developed materials, fabricated as discs (∼3.2 mm thick, 11 mm in diameter) and strips (∼3.2 mm thick, 80 × 15 mm^2), were comprehensively analyzed. Fourier-Transform Infrared Spectroscopy confirmed the successful copolymerization, as characteristic peaks corresponding to the monomers were observed. Since the development of IOL materials hinges on understanding their physical-chemical, optical, and mechanical characteristics—particularly the equilibrium water content (EWC)—our initial focus was on identifying EWC as a key factor in the development of IOLs. The results showed that the EWC value increased with higher HEA concentrations. Contact angle measurements indicated that the polymers exhibited hydrophilic behavior, with values ranging from 68 to 76°. X-ray diffraction analysis demonstrated that the HEA concentration influenced the crystalline structure, which, in turn, affected the mechanical properties. The results indicated that higher HEA concentrations, corresponding to increased EWC values (i.e. ∼8%), led to enhanced flexibility, as evidenced by a decrease in tensile strength from 1.71 to 1.13 MPa, and reduced hardness, which declined from 57.5 to 47.5 Shore A. Additionally, refractive index analyses revealed a gradual decrease with increasing HEA concentrations, ranging from 1.565 to 1.543 when measured at 480 nm and from 1.547 to 1.528 when measured at 660 nm. The evaluation of the coefficient of variation and Pearson's correlation coefficient demonstrated strong material consistency and clear trends across formulations, reinforcing the reliability of the observed properties. These findings emphasize the significance of EWC and the ratio of hydrophilic monomers in acrylic-based copolymers, suggesting that future research could benefit from designing copolymers with tailored physical-chemical, optical, and mechanical properties for IOL applications.

1. Introduction

The human eye is a complex, highly specialized organ that captures light and converts it into electrical signals, which the brain then interprets as visual images [1]. It consists of various structures, including the cornea, lens, retina, and optic nerve, each playing a crucial role in the visual process [2]. Among common ocular diseases, cataracts, which cause clouding of the lens and prevent light from reaching the retina,

not only reduce visual acuity but also significantly impact quality of life, highlighting the need for effective treatment and management strategies. Cataracts are a leading cause of blindness worldwide, affecting millions of people and significantly impairing their vision and quality of life [3]. According to the World Health Organization, cataracts account for approximately 51% of global blindness and affect about 20 million people [4]. This prevalent condition necessitates effective treatment methods to restore visual acuity and improve patients' quality of life. Cataracts are commonly treated through surgical intervention, which involves the removal of the opacified natural lens and its replacement with an artificial, transparent, disc-shaped intraocular lens (IOLs) possessing a specific refractive power. Materials used for IOLs must fulfill several critical requirements, including high optical transparency, excellent image resolution, chemical stability, outstanding biocompatibility with ocular tissues, and the ability to withstand standard sterilization procedures [5].

Research on IOL materials began in 1949, when Ridley first introduced the use of polymethylmethacrylate (PMMA) [6]. Although PMMA is a rigid material that is difficult to shape and cannot withstand elevated temperatures and pressures, it was widely used for IOLs for many years due to its optical clarity and biocompatibility [7]. However, advancements in cataract surgery techniques created a demand for softer, foldable IOL materials to allow for smaller surgical incisions and reduced postoperative complications. The first foldable IOL, fabricated from silicone elastomer, was introduced in 1976 [5]. Silicon-based IOLs were initially favored over PMMA due to their flexibility and ease of insertion [8]. Nonetheless, limitations such as pregressive loss of transparency over time and their rapid unfolding behavior – often leading to mechanical stress on the capsular bag – prompted further research into alternative materials [9]. Consequently, foldable acrylic polymers were developed, offering improved handling characteristics, optical stability, and sustained transparency. These materials remain among the most widely used IOLs in current clinical practice [10]. Acrylic materials used in IOLs are typically composed of polymers or copolymers synthesized from various monomers, including methyl acrylate, methyl methacrylate (MMA), ethyl methacrylate (EMA), 2-hydroxy EMA (HEMA), 2-hydroxyethyl acrylate (HEA), and 2-(2-ethoxy ethoxy) ethyl acrylate (EEEA). Acrylic IOLs are generally classified into two categories: hydrophilic and hydrophobic. Hydrophobic IOLs typically contain 0.5%–1% water, whereas hydrophilic IOLs exhibit a significantly higher water content, generally ranging from 18% to 38% [11]. Due to their high water content, hidrophilic IOL materials demonstrate excellent compatibility with ocular tissues [12] and have been reported to reduce the aggregation of inflammatory cells on their surface [13]. However, a study conducted by Ozyol *et al* indicated that the hydrophilic surface may promote the proliferation of lens epithelial cells, thereby increasing the risk of posterior capsule opacification (PCO) in comparison to hydrophobic counterparts [12]. On the other hand, hydrophobic IOL materials possess an adhesive surface that promotes tight adherence to the capsular bag, thereby limiting the migration and proliferation of lens epithelial cells and subsequently reducing the incidence of PCO [14]. However, a notable drawback of hydrophobic IOLs is the formation of glistenings [9] – microvacuoles that develop within the IOL material over time. Glistenings can lead to increased intraocular light scattering, resulting in glare and unintended optical aberrations, which may cause visual discomfort, particularly under low-light conditions. A commonly accepted explanation for the formation of glistenings is that water, trapped within the hydrophobic polymer matrix, forms microvacuoles as a result of temperature-induced phase separation and localized expansions [11]. To mitigate this phenomenon, increasing the water content of the material in a controlled manner has been proposed as a potential strategy to reduce glistening formation while maintaining desirable optical and mechanical properties [15]. Efforts to develop hydrophobic acrylic IOLs with reduced glistening have led to numerous studies demonstrating that controlled adjustment of the material's water content can effectively minimize glistening formation [15–17].

Since 1949, decades of research have significantly advanced the development of IOL materials. While early investigations primarily focused on identifying materials that were optically suitable, chemically stable, and biocompatible, current research efforts are increasingly directed toward optimizing material properties and fabrication techniques to meet more specific, individualized clinical requirements [18].

To regulate the water content within the biomaterial, the HEA monomer was incorporated due to its well-documented biocompatibility in ophthalmic applications, as extensively reported in the literature [19–22]. Additionally, the EEEA monomer was selected as a hydrophobic component, recognized for its reliability and favorable biocompatibility in ocular materials [23, 24]. The copolymer structure formed by combining these two monomers provides a robust foundation for achieving the intended objective of this study. Furthermore, ethylene glycol dimethacrylate (EGDMA), a widely used crosslinking agent in copolymer systems, was employed. It contains two functional groups capable of forming covalent bonds between individual polymer

chains, thereby enhancing the structural integrity and mechanical stability of the resulting material [25].

Despite advancements in IOL materials and processing techniques, significant gaps remain in the current literature. In the studies conducted by Kim *et al* the effects of copolymerizing hydrophobic and hydrophilic monomers – specifically incorporating HEA as the hydrophilic component – were investigated with respect to the physical properties of hydrophobic acrylic IOL materials. The study specifically addressed key parameters such as glistening formation, equilibrium water content (EWC), refractive index, and glass transition temperature [19, 20]. However, the literature lacks a comprehensive evaluation of how variations in water content influence the mechanical and optical properties of IOL materials. In particular, there is a notable scarcity of studies addressing the impact of water content on mechanical performance, residual monomer content, and refractive index. Moreover, the limited mechanical characterization of IOL materials hinders a thorough understanding of their functional advantages and limitations. While several studies in the literature have addressed the optical and mechanical properties of IOLs [26–28], a systematic analysis linking these properties to material water content remains largely unexplored. However, to the best of our knowledge, comprehensive mechanical testing of IOL materials has not been extensively explored or systematically investigated to date.

Therefore, this research aims to address the aforementioned gaps by systematically investigating the influence of water content on the properties of IOL materials and providing a comprehensive characterization of newly developed copolymers. While this work provides valuable insights into the structural and functional properties of the material, biological assessments were beyond the scope of the presented study. Nonetheless, this research aims to contribute to the development of more effective and reliable intraocular lenses (IOL), while also enriching the current scientific literature on IOL material characterization. Furthermore, by comprehensively investigating the key factors influencing IOL performance, this study seeks to deepen our understanding of these critical parameters and support future advancements in the medical field, particularly in the context of cataract treatment.

The novelty of this work was therefore to evaluate the physical-chemical and mechanical properties of the synthesized material, with a particular focus on its suitability for IOL applications. To achieve this, a series of characterization techniques were employed, including Fourier-Transform Infrared Spectroscopy (FTIR), residual monomer content analysis, EWC, contact angle (CA) measurements, x-ray diffraction (XRD), mechanical testing in accordance with ISO standards, and refractive index determination. These analyses were conducted to assess the effects of HEA monomer concentration and associated water content on the overall performance of the copolymer system.

2. Materials and methods

2.1. Materials

EEEA and HEA (96.0%) were purchased from Sigma-Aldric and used as hydrophobic monomer and hydrophilic monomers, respectively. As radical polymerization initiator, UV-light blocker, and cross-linker, Azobis Iso Butyro Nitrile (AIBN), 2-(2′-Hydroxy-5′ methacryloxy ethyl PHENYL)-2 H-benzotriazole (UV-090), and EGDMA were selected and bargained from Sigma-Aldrich. Phosphate buffer saline (PBS)-(Sigma-Aldrich) was utilized in the preparation, hydration, and storage steps.

2.2. Thermal copolymerization of EEEA and HEA

Thermal copolymerization is a fundamental process in polymer chemistry used to create copolymers with desirable physical and chemical properties by combining different monomers [29]. This article explores the thermal copolymerization of acrylates, specifically EEEA and HEA monomers, which were chosen for their unique properties. EEEA is a monomer with a long ethoxy chain that imparts flexibility and improved solubility in various solvents. Its ethoxy groups make it suitable for applications requiring low glass transition temperatures (T_g). HEA contains a hydroxyl group that makes it highly reactive and ideal for post-polymerization modifications. This functionality allows for crosslinking and bonding with other polymer chains or additives, enhancing the mechanical strength and chemical resistance of the final copolymer.

The process involved initiating the reaction between EEEA and HEA in the presence of AIBN as a thermal initiator. AIBN decomposes upon heating to generate free radicals, which initiate polymerization by attacking the double bonds in the acrylate monomers, forming reactive sites. The reactive sites on the monomers continue to react with other monomer molecules, creating a growing polymer chain [30]. The random addition of EEEA and HEA units to the chain results in a copolymer with properties derived from both monomers. The polymerization process is terminated by combining two reactive chain ends. The resulting copolymer has a defined molecular weight and a distribution of EEEA and HEA units. The ratio of EEEA to HEA affects the copolymer's properties, such as flexibility, hydrophilicity, and potential for post-polymerization modifications. A higher EEEA content results in a more flexible and hydrophilic copolymer, while a higher HEA

Table 1. Prepared copolymers with different HEA and EEEA monomer ratios.

Formulations	F1	F2	F3	F4	F5	F6	F7	F8
HEA concentration [wt.%]	3.5	7.00	10.5	14.00	17.5	21.00	24.5	28
EEEA/HEA ratio [%]	27.5	13.2	8.5	6.1	4.7	3.7	3	2.5

content increases the potential for crosslinking and chemical resistance.

The copolymers were synthesized using a casting mold method. Solutions containing EEEA, HEA, 3.1 wt% EGDMA as a crosslinking agent, and 0.5 wt% AIBN as the initiator were prepared and poured into polypropylene molds. These molds were then placed in a vacuum oven and subjected to thermal polymerization at 75 °C under a pressure of 50 mbar for 20 h. Following polymerization, the samples were cooled to 35 °C for 1.5 h under the same pressure to complete the curing process. The resulting copolymers were stored in PBS for subsequent analysis. The hydrated samples, with a thickness of ∼3.20 mm, were cut into discs with a diameter of 11.00 mm or into strips measuring ∼80 × 15 mm^2, using a manual cutting press.

In this study, eight different copolymers with varying EEEA to HEA ratios were prepared, and their mechanical, thermal, and optical properties were compared. EEEA is a hydrophobic polymer, whereas HEA is a hydrophilic one. Our goal was to develop a primarily hydrophobic material with a controlled and minimal amount of water content to introduce hydrophilic properties. Through the copolymerization process, EEEA remained the dominant polymer, while the concentration of HEA gradually increased from 3.5% to 28% (refer to table 1), with the concentration of EEEA decreasing proportionately. The concentration range was chosen to effectively balance the hydrophobic and hydrophilic properties. At lower concentrations (3.5%), HEA minimally affects the water content, ensuring that the material remains hydrophobic. As the HEA concentration increases up to 28%, the material gradually becomes more hydrophilic without significantly compromising its overall hydrophobicity. This controlled variation enables precise adjustment of the water content in the final material.

The polymerization temperature influences the rate of reaction and the molecular weight of the resulting copolymer. Higher temperatures generally increase the reaction rate but can result in lower molecular weight due to an increase in termination events. Therefore, the reaction temperature was kept constant for all formulations. Likewise, the concentration of the thermal initiator affects the initiation rate, and the number of polymer chains formed. Higher initiator concentrations produce more polymer chains with lower molecular weights, while lower concentrations yield fewer chains with higher molecular weights. To eliminate the initiator effect on the prepared formulations, the AIBN concentration was kept constant across all samples.

Table 2. High-performance liquid chromatography gradient system.

Gradient: time (min)	A[a] (%)	B[b] (%)
0	5	95
1	5	95
11	100	0
17	100	0
18	5	95
22	5	95

[a] Mobile phase A: acetonitrile LC grade.
[b] Mobile phase B: water LC grade.

Table 3. Compound retention times.

Compound	Retention time (min)
HEA	8.6
EEEA	11.5
EGDMA	13.8

2.3. FTIR analysis

Chemical analysis of the prepared copolymers was conducted employing a spectrophotometer (Shimadzu, IRPrestige21, Japan). The analysis encompassed a scanning range of 4000−500 cm^{-1} at room temperature (RT) to confirm the correct copolymerization of the samples.

2.4. Monomer residue

For the monomer residue test, the following materials are required in addition to standard laboratory equipments: analytical balance with a precision of 0.01 mg; laboratory vortex; and a membrane filter for sample filtration, e.g. regenerated cellulose (RC) with 0.45 μm pore size. All analysis were performed on a Shimadzu high-performance liquid chromatography (HPLC) system equipped with a diode array detector. Reversed-phase Hi-Crom Alltima C18 (250 × 4.6 mm, 5.0 μm) column was utilized. The injection volume was set up at 10 μl, and detection was performed at 254 nm. The oven temperature was set to 25 °C. The mobile phase is the gradient water and acetonitrile with a flow rate fixed at 0.7 mL min^{-1} . Residual monomers were analyzed using a HPLC system with gradient flow involving two different mobile phases (see table 2).

The retention times for HEA, EEEA, and EGDMA are given in table 3.

2.5. EWC studies

The EWC test was performed for all eight formulations. Briefly, three samples for each formulation were dried at 50 °C for 48 h and weighed. Next, the samples were left in an isotonic saline solution for 72 h. EWC was calculated by reweighing the samples at the end of 24, 48, and 72 h, using the following formula (1):

$$\text{Water Content} = \left(1 - \frac{W1}{W2}\right) \times 100 \qquad (1)$$

where W_1 and W_2 denote average weights before and after hydration.

2.6. Contact angle measurements

Polymeric networks often exhibit varying degrees of hydrophobicity or hydrophilicity, which are commonly assessed through CA measurements. The CA (generally represented by θ_C) is defined as the angle between the tangent to the liquid–vapor interface and the solid surface at the three-phase contact line. This involves capturing video footage of a water droplet on a solid surface and analyzing the resulting images to determine the CA through a fitting process. In this study, CAs of the prepared samples were measured using the Drop Shape Analyzer System DSA 10 Mk2 (Kruss, Germany), operated under ambient humidity and temperature conditions. Droplets of deionized water, approximately 2.0 µl in volume, were carefully deposited onto the sample surface for analysis. For each formulation, three tests were performed on different areas, and no significant differences were observed between consecutive measurements on the same sample.

2.7. XRD analysis

The samples were investigated in Bragg-Brentano geometry using a Shimadzu—LABX | XRD-6100 x-ray diffractometer (Shimadzu, Japan). The tests were conducted using 40 kV voltage and 30 mA current, with a scanning rate of $2°\text{min}^{-1}$. The XRD patterns were collected in the range $2\theta = 10–80°$.

2.8. Mechanical characterization

2.8.1. Tensile testing

To evaluate the tensile properties of the eight different formulations, three samples from each formulation were prepared. The test was performed on the Lloyd LS5 universal testing machine (Ametek Inc., USA), equipped with a 100.00 N load cell. The specimens were cut into dog-bone shapes using a manual cutting press in accordance with the ISO 527–2 standard, yielding final dimensions of 3.20 mm in thickness, 10.00 mm in width, and 75.00 mm in overall length. The dimensions of the samples were carefully measured at RT, using a digital caliper (Mitutoyo Corp., Japan) and a micrometer (Mitutoyo Corp., Japan) to ensure compliance with the standard requirements. Prior to testing, all samples were immersed in a saline solution at a temperature of 35 °C ± 2 °C and a relative humidity of 50% ± 5% for at least 72 h to reach EWC. According to the used standard, the samples were subjected to a constant deformation rate of 5 mm min^{-1} until failure occurred. During the tensile tests, the applied force and the corresponding elongation of the specimens were continuously recorded.

2.8.2. Hardness testing

Hardness measurements were conducted using an LXD Shore A hardness tester (Loyka, Turkey). The hardness of three samples from each formulation was measured according to the ISO 868 standard, using samples with dimensions of 10.00 mm in width, 10.00 mm in length, and 3.20 mm in thickness. All samples were prepared using a manual cutting press and were measured at RT. The dimensions of the samples were carefully measured using a digital caliper (Mitutoyo Corp., Japan) and a micrometer (Mitutoyo Corp., Japan) to ensure compliance with the standard requirements. Prior to testing, all samples were immersed in a saline solution at a temperature of 35 °C ± 2 °C and a relative humidity of 50% ± 5% for at least 72 h to reach EWC. The hardness values were recorded in Shore A units.

2.9. Refractive index measurement

Refractive index was measured using a fully automatic spectral refractometer (SCHMIDTHAENSCH ATR L, Germany), at a controlled temperature of 37 °C. The device is capable of measuring refractive index from thin solid materials. For the measurement, samples of each formulation were cured in disc form with a diameter of 11 mm and a thickness of 1 mm. The disc samples were placed into the measurement chamber using a pressing tool, and the test was initiated. For each formulation, three samples were measured.

2.10. Statistical analysis

The results of water CA measurements, mechanical testing, and refractive index investigations were analyzed using statistical models to assess variability, correlation, and consistency across different formulations. The coefficient of variation (CV) was calculated for each dataset to evaluate the relative dispersion of values. Pearson's correlation coefficient (R^2) was utilized to evaluate relationships between wettability, mechanical, and optical properties. Descriptive statistics, including mean and standard deviation, were computed for all tests to ensure reproducibility and reliability.

Linear regression analysis was conducted to identify trends within the data, particularly in mechanical properties, such as elongation at break and

tensile strength, as well as refractive index measurements across different wavelengths. Where applicable, statistical significance was determined to validate observed correlations and material performance trends, ensuring a robust interpretation of the results.

3. Results and discussion

3.1. FTIR

FTIR analysis was employed to confirm the presence of specific chemical bonds and functional groups, thereby verifying the successful synthesis of the targeted copolymer structure.

Figure 1 shows the FTIR spectra of the HEA and EEEA monomers, as well as the poly(HEA/EEEA) copolymer. While eight formulations were prepared, the spectra of the first three formulations (F1, F2, and F3) were selected for comparison with the monomer spectra. This selection was made because all formulations were the same, and including the spectra of the other formulations would be repetitive. As depicted in the spectrum of the HEA monomer, a broad peak is observed between 3300 and 3600 cm^{-1}, attributable to the presence of the hydroxyl group [31].

In the EEEA monomer spectrum, distinct peaks are present at 2850−2950 cm^{-1}, corresponding to the C−H stretching vibrations of the ethoxy groups. The ester carbonyl group shows a sharp peak in both monomers in 1730−1750 cm^{-1} [32]. In the FTIR spectra of the poly (HEA/EEEA) copolymer formulations (F1, F2, and F3), the characteristic peaks from both monomers are evident. The broad O−H stretching band between 3300 and 3600 cm^{-1} confirms the incorporation of HEA into the copolymer. The C−H stretching peaks at 2850−2950 cm^{-1} are also present, indicating the contribution of the EEEA monomer. The strong carbonyl stretching peak at around 1735 cm^{-1} confirms the presence of ester groups from both monomers in the copolymer. Additionally, peaks between 1050 and 1150 cm^{-1}, corresponding to the C−O−C stretching vibrations, further verify the integration of EEEA [33].

The spectra demonstrates that the copolymerization process successfully integrates the unique functional groups of both HEA and EEEA monomers, resulting in a copolymer with combined properties. Variations in peak intensities among F1, F2, and F3 reflect different ratios of HEA to EEEA, correlating with the expected changes in copolymer flexibility, hydrophilicity, and potential for post-polymerization modifications.

In a similar study by Oucif *et al* various ratios of HEA were successfully polymerized with HEMA using free radical polymerization [22]. The hydrogels within the study were synthesized through the simultaneous copolymerization and cross-linking of HEMA and HEA co-monomers in seven different ratios for therapeutic soft contact lens (SCL) applications. The copolymers' microstructures were examined using FTIR spectroscopy. As anticipated, all the hydrogels' spectra displayed a broad band in the hydroxyl region centered at 3360 cm^{-1}, indicating hydrogen bonding associations between the hydroxyl and carbonyl groups of the HEA and HEMA ester groups. Moreover, the FTIR spectra of the hydrogels were mainly characterized by a carbonyl peak at 1720 cm^{-1}, indicating the vibration of the ester carbonyl groups. Additionally, a shoulder at 1580 cm^{-1} appeared, which resulted from the association of carbonyl groups with hydroxyl groups through hydrogen bonding, confirming the formation of the copolymer.

In another study, copolymerization was employed to create various functional copolymers of HEA and MMA, denoted as HEMMA (copolymer of HEA and MMA) [34]. For this, AIBN was used as the initiator and dimethylformamide served as the solvent in a solution polymerization process. The FTIR spectra analysis revealed a decrease in the signal at 3416 cm^{-1} (C−OH bond) with the reduction of HEA units in the copolymers, indicating differences in the repetitive units of HEA and MMA within the HEMMA copolymers. Additionally, no HEMMA copolymer exhibited a signal at 1638 cm^{-1} (stretching of −CH=CH−), suggesting that all monomers had reacted or that any residual monomers were removed during the purification process of the HEMMA copolymers.

3.2. Residual monomer

The quantification of residual monomer content was conducted to evaluate the efficiency of polymerization and to detect unreacted species that may compromise further biocompatibility testing.

All three monomers were dissolved in ethyl acetate and injected into the HPLC system. Monomer standards were prepared with ethyl acetate at concentrations of 20%, 50%, 100%, 120%, and 150%. The HPCL chromatograms of 100% standard monomers are shown in figure 2(a). The results show that monomer resolution is acceptable to proceed with the analysis. Figure 2(b) shows the corresponding monomer peak areas characterized by different standard solutions. Monomer standard areas were used to construct calibration curves for each monomer. Different calibration curves for each monomer were shown in figures 2(c)–(e). Linearity graphs were plotted for each standard; it was determined that the correlation coefficients from the graph curves were 0.999.

Subsequently, an extraction setup was established for each formulation. Each formulation was homogenized, divided into equal parts, and then extracted with ethyl acetate in the extraction setup. The extraction products were injected into an HPLC device.

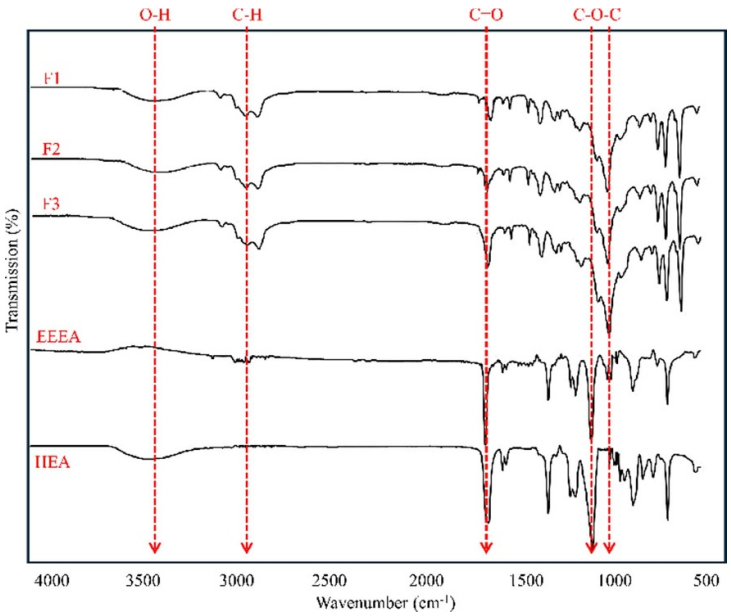

Figure 1. FTIR spectra of 2-hydroxy ethyl acrylate (HEA) and 2-(2-ethoxy ethoxy) ethyl acrylate (EEEA) monomers, and copolymers of formulations F1, F2, and F3.

In the residual monomer analysis conducted on the formulations, no monomers were detected in the residual matrix injected into the HPLC system.

As illustrated in figure 3, the HPLC output for F1 only displayed a peak corresponding to the solvent ethyl acetate, with no additional peaks observed.

From the results, no monomer residues were found in the formulations. Although, it was noted that some different residues (i.e. oligomers) were detected in the HPLC system.

Residual monomers have been detected and measured in other studies using a HPLC device [35, 36]. In addition to HPLC, instrumental devices such as Gas Chromatography/ Mass Spectrometry (GC-MS) have been used to detect residual monomers [37]. Some studies have also employed HPLC devices in the measurement of low-density polymers [38].

3.3. EWC

Swelling experiments were performed to determine the copolymer's equilibrium water uptake, offering insights into its hydration capacity and its relevance to intraocular optical performance.

Figure 4 depicts the EWC as a function of HEA concentration (wt.%) for three different time intervals: 24 h, 48 h, and 72 h. The data demonstrates a positive correlation between HEA concentration and EWC, with higher HEA concentrations resulting in increased water content across all time intervals.

For the 24 h interval (blue line), the EWC starts at approximately 2.0% for the lowest HEA concentration and rises steadily to around 8.0% at the highest concentration. The 48 h interval (orange line) shows a similar trend, with slightly higher EWC values compared to the 24 h data, indicating further water absorption over time. The 72 h interval (green line) exhibits the highest EWC values, beginning at around 2.5% and reaching nearly 9.0%, highlighting the continued water absorption with prolonged exposure.

The observed increase in EWC with higher HEA concentrations can be attributed to the hydrophilic nature of the hydroxyl groups present in HEA, which enhances the copolymer's ability to absorb water. Additionally, the prolonged time intervals allow for more significant water uptake, demonstrating the time-dependent nature of the EWC in HEA/EEEA copolymers. This behavior is consistent with the hydrophilic and reactive properties of HEA, making these copolymers suitable for applications requiring enhanced water absorption and retention. In this respect, Kim *et al* showed the effect of hydrophilic monomer relation with water content [20]. In their study, they found that the water content increases with a higher proportion of hydrophilic monomers. Specifically, as the monomer ratio increased from 0% to over 20%, the water content rose from 1% to more than 2%.

3.4. Contact angle measurements

Static CA measurements were utilized to assess surface wettability, providing information on hydrophilicity/hydrophobicity with implications for protein adsorption and cellular response.

Figure 5 illustrates the CA measurements of water droplets on the surface of poly(HEA/EEEA) copolymers as a function of HEA concentration (wt.%).

The CA indicates surface hydrophilicity, with lower angles signifying more hydrophilic surfaces.

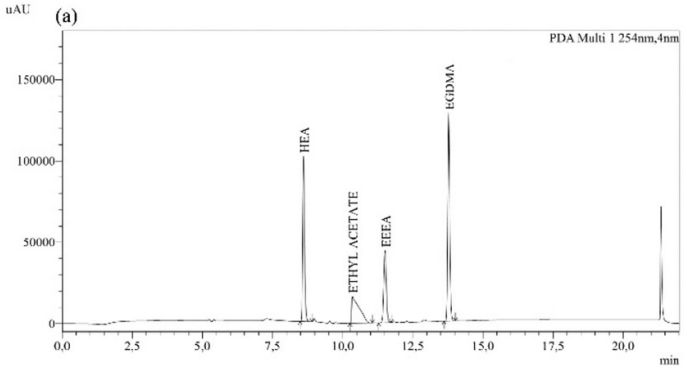

(b)

Standarts (%)	IIEA	EEEA	EGDMA
20	87241	54930	128391
20	87186	54823	128320
50	224739	140149	328478
50	225276	140043	327965
100	451736	281342	658772
100	451745	281007	659544
120	537564	334270	784233
120	537672	334325	782867
150	668931	416038	974673
150	669632	416406	976113

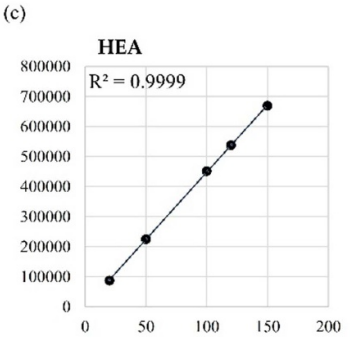

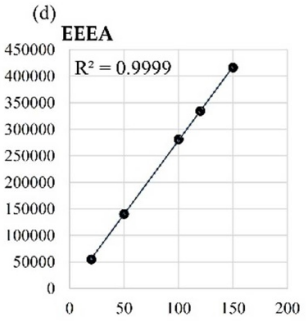

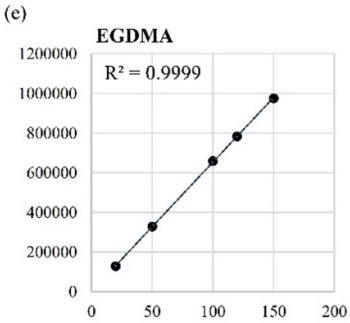

Figure 2. (a) High-performance liquid chromatogram (HPLC) showing each monomer injected into the HPLC system at 100% standard concentration; (b) peak areas of monomers with varying concentrations; (c) linearity graph of hydroxyethyl acrylate monomer; (d) linearity graph of 2-ethoxyethoxyethyl acrylate monomer; (e) linearity graph of ethylene glycol dimethacrylate monomer. R^2 represents the determation coefficient.

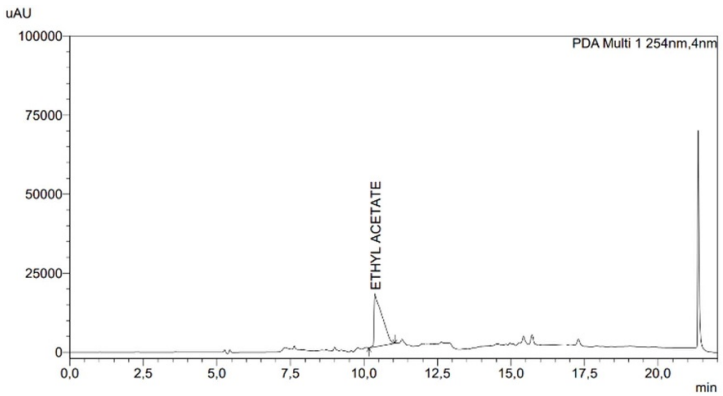

Figure 3. High-performance liquid chromatogram of the first injection of formulation 1.

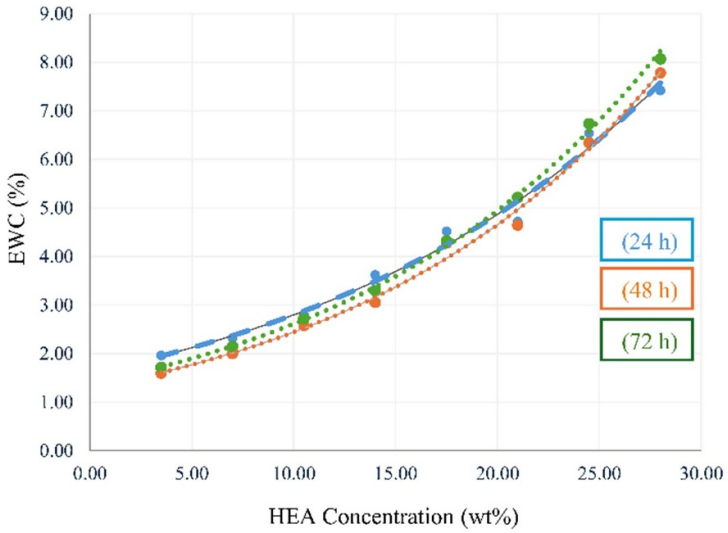

Figure 4. Equilibrium water content (EWC) relation in respect to HEA concentration for 24 h, 48 h, and 72 h.

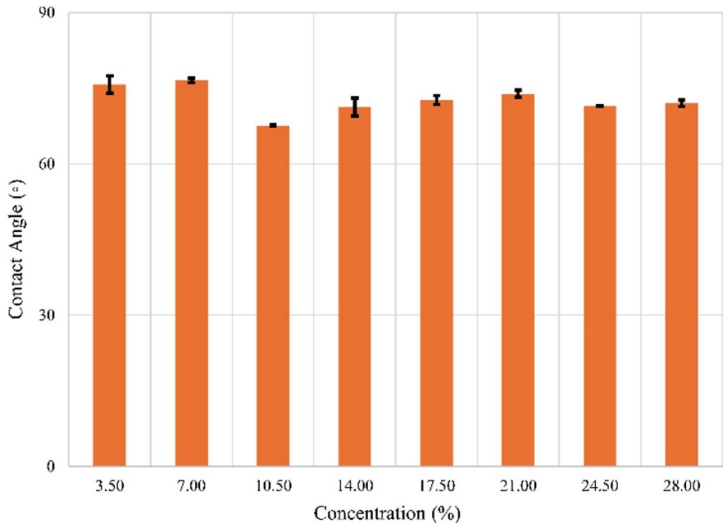

Figure 5. Contact angle of water droplets on the surface of poly 2-hydroxy ethyl acrylate/2-(2-ethoxy ethoxy) ethyl acrylate (HEA/EEEA) copolymers versus HEA concentration (wt.%). Data reported as mean ± standard error ($n = 3$).

At 3.5% HEA concentration, the CA is approximately 75°, suggesting a hydrophilic surface. As the HEA concentration increases to 7%, the CA remains around 76°, indicating minimal change in hydrophilicity at this low HEA content. When the HEA concentration reaches 10.5%, the CA decreases to about 68°, reflecting an increase in surface hydrophilicity. This trend continues as the HEA concentration increases to 14%, with the CA around 70°, and remains fairly constant at 71° for HEA concentrations of 17.5%, 21.0%, 24.5%, and 28%, indicating a stable hydrophilic nature.

Overall, the relationship between HEA concentration and water CA showed no significant changes. The average CA values across concentrations from 3.5% to 28% showed minor fluctuations, with the highest being 76.85° at 7% and the lowest being 67.5° at 10.5%. Within the tested range, HEA concentration does not have a significant impact on the surface's wettability, suggesting stable surface characteristics irrespective of HEA concentration. One should emphasize that the CA measurements demonstrated high consistency across all formulations, exhibiting a CV ranging from 0% to 2.7% and an R^2 value of 0.89 when assessing CA variations. These findings further confirm the stability of the surface wettability properties.

A study conducted with varying concentration of hydrophilic monomers (i.e. HEA, HPA, HBA, and HEMA) showed that the CA values gradually

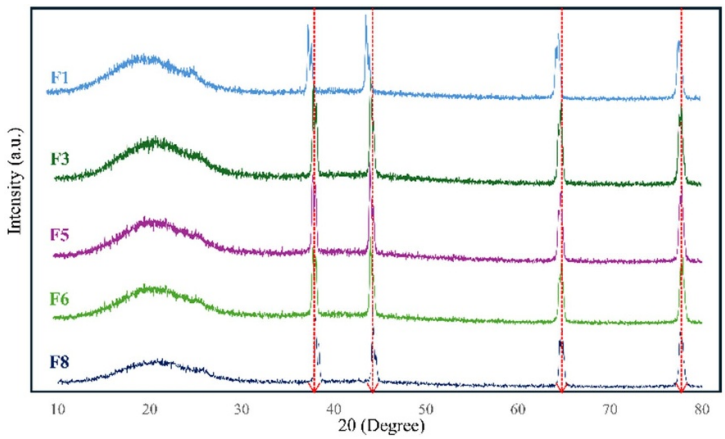

Figure 6. X-ray diffractograms of copolymer formulations with different 2-hydroxy ethyl acrylate (HEA) concentrations.

decreased when the HEA concentration raised from 0 to over 20% [20]. The study demonstrated that the HEA monomer significantly reduced the water CA at low concentrations (i.e. 0%−2%), enhancing surface hydrophilicity. This contrasts with our findings where no significant changes were observed from 3% to 28%. Understanding the exact reasons behind these differences requires further investigation into concentration ranges, polymer matrix compositions, and experimental conditions.

3.5. XRD

XRD analysis was used to assess the degree of crystallinity and amorphous content in the copolymer, facilitating interpretation of its molecular organization in relation to mechanical and optical characteristics.

Figure 6 presents the XRD patterns selected formulations (F1, F3, F5, F6, F8) of poly (HEA/EEEA) copolymers with varying HEA concentrations. Due to the repetitive pattern in all formulations, only five formulations were presented. Each diffractogram displays characteristic peaks that correspond to the crystalline structures of the copolymers. The XRD patterns reveal distinct peaks at specific 2θ values, indicating the presence of crystalline phases within the copolymer matrix. The intensity of these peaks varies with the concentration of HEA, reflecting changes in the degree of crystallinity. At lower HEA concentrations, the peaks are more pronounced, suggesting a higher degree of crystallinity. As the HEA concentration increases, the peak intensities decrease, indicating a reduction in crystallinity. This trend is consistent across all samples, with the most significant peaks observed at approximately the same 2θ positions. The reduction in peak intensity with increasing HEA content suggests that higher concentrations of HEA disrupt the regularity of the polymer chains, leading to a more amorphous structure.

These XRD results complement the FTIR and CA data, underscoring the impact of HEA on the physical properties of the copolymers. The decrease in crystallinity with increasing HEA content aligns with the observed increase in hydrophilicity and EWC, confirming the role of HEA in modifying the structural and surface properties of the copolymers. A similar relationship was also observed in a study investigating the addition of polyhedral oligomeric silsesquioxane (POSS) to PMMA lens material [39]. In contrast to our study, the addition of hydrophobic POSS group increased the intensity of the XRD peaks, creating crystalline structures to enhance the hydrophobic properties of the material. In another study, the surface properties of (i) PMMA, (ii) HEMA2-g-PMMA, (iii) HEMA3-g-PMMA materials were designed to reduce platelet adhesion [40]. As a result, the HEMA-modified materials significantly decreased platelet adhesion. These modifications, along with similar studies, are valuable for designing more versatile copolymers by integrating the best traits of the monomers.

3.6. Mechanical tests

3.6.1. Elongation at break and tensile strength

Uniaxial tensile testing was carried out to quantify the elastic modulus, tensile strength, and elongation at break, thus evaluating the mechanical robustness required for intraocular lens implantation.

The effect of EWC on the elongation at break and tensile strength of the samples is shown in figure 7. As observed, changes in the EWC of the samples resulted in a nonlinear effect on the mechanical properties. This phenomenon is consistent with similar studies in literature [41–45]. At 1.7% EWC, the elongation at break was 68.4%, and the tensile strength was 1.71 MPa. These values indicate that the polymer is flexible at low EWC. As the EWC increased from 1.7% to 3.2%, the elongation at break varied between

(a)

Formulations	Water Content (%)	Tensile Strength (MPa)	Elongation at Break (mm)
F1	1.718	1.71	68.4
F2	2.147	1.60	64.0
F3	2.728	1.69	67,9
F4	3.298	1.72	68.9
F5	4.326	1.60	64.3
F6	5.217	1.07	43.0
F7	6.736	1.41	56.7
F8	8.072	1.13	45.6

(b)

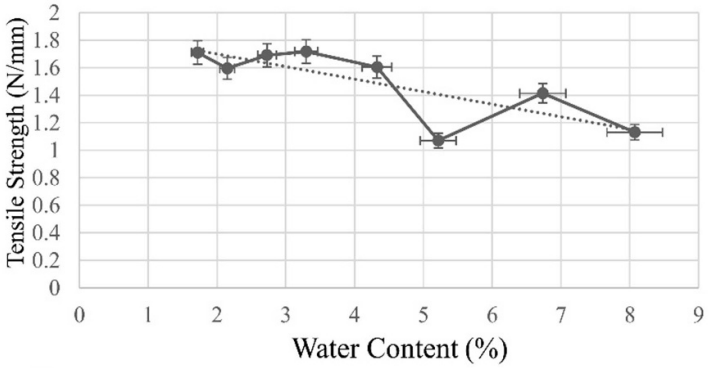

(c)

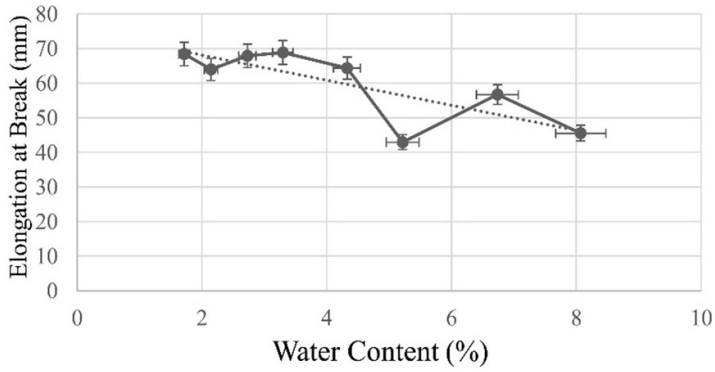

Figure 7. (a) Comparison of the inferred values of water content, tensile strength, and elongation at break for investigated formulations. (b) Tensile strength as a function of water content. (c) Elongation at break as a function of water content. Data reported as mean ± standard error ($n = 3$).

63.9% and 68.8%, and the tensile strength ranged from 1.59 MPa to 1.71 MPa. This finding aligns with results from Yin *et al* [44], which demonstrated that polymers maintain flexibility even at low moisture levels. When the EWC increased from 4.3% to 5.2%, a decrease in elongation at break and tensile strength was observed. This decrease indicates that the increase in EWC significantly reduces the mechanical properties of the samples. The significant drop at same point can be explained by the breaking of hydrogen bonds within the microstructure of the samples, leading to a weakening of their mechanical properties. As the EWC of the samples increased from 5.2% to 6.7%, a noticeable increase was observed in both tensile stress and elongation at break, with elongation at break reaching 56.7% and tensile stress reaching 1.41 MPa. This increase suggests that the samples partially regained flexibility as they adapted to the higher EWC. However, when the EWC increased to 8%, both elongation at break and tensile strength decreased again. This result indicates that the mechanical properties of the samples were initially disrupted by water

(a)

Formulations	Water Content (%)	Hardness (Shore A)
F1	1,718	57,5
F2	2,147	55,0
F3	2,728	52,5
F4	3,298	52,5
F5	4,326	52,5
F6	5,217	50,0
F7	6,736	47,5
F8	8,072	47,5

(b)

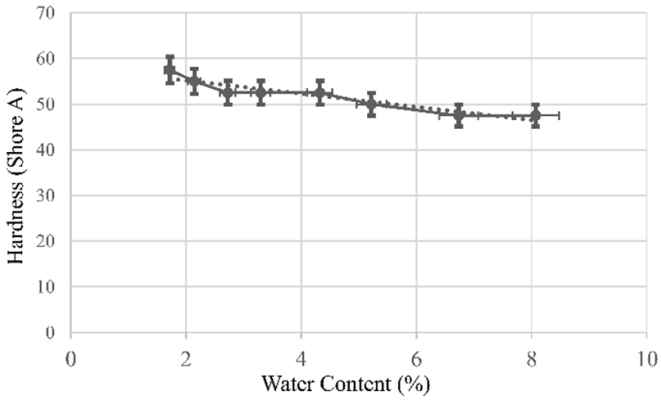

Figure 8. The effects of equilibrium water content (EWC) on the hardness values of the investigated formulations (F1—F8): (a) table with precise results. (b) Graphic of hardness *vs*. EWC. Data reported as mean ± standard error ($n = 3$).

absorption, partially recovered once the EWC stabilized, and subsequently impaired as the EWC continued to rise. This observation is consistent with various research findings. Thus, specific studies have shown that water absorption can have both beneficial and detrimental effects on the mechanical properties of polymers. In this context, research by Hamdan *et al* on hybrid-reinforced polyester composites revealed that initial water absorption could enhance flexibility, but excessive water led to significant degradation of mechanical properties [46].

In some cases, polymers may exhibit temporary improvements in mechanical properties after the initial drop due to adaptation to absorbed water. This adaptation can increase flexibility up to a certain point, but further increases in water content typically led to mechanical deterioration. Zhang *et al* study on poly (acrylic acid/acrylamide) hydrogels supports this view, noting that while initial water absorption can enhance mechanical properties through swelling, excessive water content eventually causes structural damage and performance degradation [45]. These studies indicate that while EWC can temporarily improve the flexibility of polymers by acting as a plasticizer, prolonged exposure or higher water levels can degrade the polymer matrix and reduce mechanical properties.

In conclusion, the effect of EWC on elongation at break and tensile strength is not linear. Variations in EWC result in sudden changes and fluctuations in the mechanical properties of the samples. The polymer's sensitivity to EWC appears to vary, with critical thresholds present within specific ranges. This underscores the complex influence of hydrogen bonds formed by water molecules in the polymer matrix on its mechanical properties. Additionally, one should note that the tensile strength and elongation at break measurements followed the expected mechanical behavior, with formulations exhibiting higher elongation at break also demonstrating greater tensile strength ($R^2 = 0.87$). The standard deviations for tensile strength ranged from 0.03 to 0.14 N mm^{-1}, while those for elongation at break varied between 0.10 and 1.2 mm. The CV values ranged from 2.8% to 7.6%, indicating moderate intra-sample variability.

3.6.2. Hardness testing

Surface hardness measurements were performed to determine the material's resistance to mechanical damage such as scratching and deformation, essential for long-term durability in ocular environments.

The effects of EWC on the hardness values of the samples are shown in figure 8. As the EWC increased from 1.7% to 8.0%, notable changes in hardness were

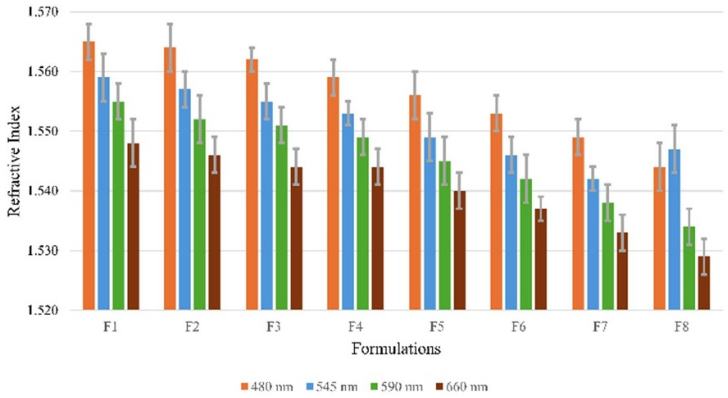

Figure 9. Refractive index values of the investigated formulations (F1—F8). Data reported as mean ± standard error ($n = 3$).

observed. Specifically, as the EWC rose from 1.7% to 2.1%, hardness decreased from 57 Shore A to 55 Shore A. Further increasing the EWC to 2.7% resulted in a reduction in hardness to 52.2 Shore A. Between 2.7% and 4.3% EWC, there was a significant change in hardness values, which then remained constant. This balance may be attributed to a more homogeneous distribution of water molecules within the polymer matrix and a reduction in the plasticizing effect. However, when EWC increased from 4.3% to 5.2% and then to 6.7%, the Shore A hardness began to decrease again. At a EWC of 8%, the decreasing trend continued, reaching a value of 47.5 Shore A. It is important to note that the Shore A hardness values exhibited a CV of approximately 3.5% and an R^2 value of 0.91 when comparing hardness across different formulations, indicating consistent and stable material hardness.

In conclusion, studies in the literature indicate that increasing EWC weakens the intermolecular interactions within the polymer matrix, leading to a decrease in the hardness of the polymers [47]. Another study suggests that water molecules interact with polymers to increase intermolecular mobility, resulting in greater flexibility [48]. Considering these findings, the plasticizing effect of EWC on polymers affects their mechanical properties, as evidenced by both existing literature and our Shore A hardness tests.

3.7. Refractive index

The refractive index of the copolymer was measured to validate its optical transparency and to ensure compliance with the designed focal requirements of IOLs.

Figure 9 shows the refractive index measurements taken at 480, 545, 590, and 660 nm. The results indicate a negative correlation between refractive index and HEA concentration, which is expected as an increase in EWC causes the refractive index to approach that of water. Also, Kim *et al* demonstrated a similar relationship between HEA concentration and refractive index [20]. In another study, the crosslinker concentration was adjusted to control the EWC in a acrylamide and methacrylamide-based copolymer material [49].

It is important to mention that the refractive index measurements exhibited minimal variation, with CV values ranging from 0.13% to 0.26%, indicating high measurement consistency. Correlation analysis revealed an R^2 value of 0.94 between refractive index measurements across different wavelengths, demonstrating strong internal consistency.

These findings could be beneficial for transparent contact or IOL materials, as a higher refractive index allows for a thinner lens. Lens thickness is crucial for IOLs since they are inserted into the eye by folding. Thinner designs may reduce potential complications during insertion. For contact lenses, thinner lenses improve oxygen diffusion and reduce friction between the eye and the eyelid.

4. Conclusions

In this work, acrylic-based copolymer formulations were synthesized by incorporating different ratios of hydrophilic HEA monomer to enhance the water intake and adjust the copolymer's mechanical characteristics. Fourier-Transform Infrared Spectroscopy verified the successful copolymerization by displaying characteristic peaks of both monomers in the prepared samples. The analysis for residual monomers confirmed that there are no unreacted monomers present, indicating high purity of the copolymers.

The EWC studies demonstrated that higher concentrations of HEA result in increased water absorption, revealing the hydrophilic nature of HEA. Contact angle measurements indicated that surface hydrophilicity did not correlate with higher HEA content. X-ray diffraction showed that the incorporation of HEA affects the crystalline structure of the copolymers, potentially influencing their

mechanical properties. Copolymers with higher HEA content exhibited enhanced flexibility and reduced hardness, indicating improved mechanical performance.

Refractive index measurements showed a negative correlation between refractive index and HEA concentration, as increasing EWC causes the refractive index to approach that of water. These insights are crucial for optimizing the performance and functionality of copolymers in IOLs.

Overall, this study highlights the critical role of EWC and monomer ratio in determining the properties of acrylic-based copolymers. Optimizing these parameters can lead to the development of more effective and reliable IOL materials, ultimately improving outcomes for patients undergoing cataract surgery. Future research should focus on further exploring the impact of EWC on the long-term performance, potential toxic effects, and biocompatibility of these materials. Additionally, exploring other copolymer systems could provide valuable insights for the development of advanced ophthalmic applications.

Data availability statement

All data that support the findings of this study are included within the article (and any supplementary files).

Acknowledgment

L. D. acknowledges support from the Romanian Ministry of Education and Research, under Romanian National Nucleu Program LAPLAS VII–contract No. 30N/2023. M. E. R. acknowledges The Scientific and Technological Research council of Turkey (TUBITAK) 2244 Industrial PhD. Program (Grant ID: 118C146) for the scholarship. D. A also extends his thanks to the Council of Higher Education (YÖK) 100/2000 program for their assistance.

References

[1] Roy S and Nagrale P 2022 *Cureus* **14** e30125
[2] Durak S, Rad M E, Yetisgin A A, Sutova H E, Kutlu O, Cetinel S and Zarrabi A 2020 *Nanomaterials* **10** 1191
[3] Khairallah M *et al* 2015 *Investig. Ophthalmol. Vis. Sci.* **56** 6762
[4] Forrest S L, Mercado C L, Engmann C M, Stacey A W, Hariharan L, Khan S and Cabrera M T 2023 *Glob. Health Sci. Pract.* **11** E2200091
[5] Allarakhia L, Knoll R L and Lindstrom R L 1987 *J. Cataract Refract. Surg.* **13** 607
[6] Ridley H 1952 *Br. J. Ophthalmol.* **36** 113
[7] Apple D J, Mamalis N, Loftfield K, Googe J M, Novak L C, Kavka-VAN Norman D, Brady S E and Olson R J 1984 *Surv. Ophthalmol.* **29** 1
[8] Kapoor S and Gupta S 2020 *Basic Science of Intraocular Lens Materials* (Intraocular LensIntechOpen)
[9] Čanović S, Konjevoda S, Pavičić A D and Stanić R 2019 *Intraocular Lens (IOL) Materials* (Intraocular Lens. IntechOpen)
[10] Olson R J, Mamalis N, Werner L and Apple D J 2003 *Am. J. Ophthalmol.* **136** 146
[11] Werner L 2021 *Ophthalmology* **128** e74
[12] Ozyol P, Ozyol E and Karel F 2017 *Turk. J. Ophthalmol.* **47** 221
[13] Abela-formanek C, Amon M, Kahraman G, Schauersberger J and Dunavoelgyi R 2011 *J. Cataract Refract. Surg.* **37** 104
[14] Katayama Y, Kobayakawa S, Yanagawa H and Tochikubo T 2007 *Ophthalmic Res.* **39** 276
[15] Tetz M and Jorgensen M R 2015 *Curr. Eye Res.* **40** 969
[16] Packer M, Fry L, Lavery K T, Lehmann R, McDonald J, Nichamin L, Bearie B, Hayashida J and Altmann G E 2013 *Clin. Ophthalmol.* **7** 1905
[17] Stanojcic N, O'Brart D, Hull C, Wagh V, Azan E, Bhogal M, Robbie S and Li J P O 2020 *J. Cataract Refract. Surg.* **46** 986
[18] Dick H B and Gerste R 2021 *Ophthalmol.* **128** e206
[19] Kim T H, Ko B Y and Song K C 2024 *Int. J. Polym. Mater. Polym. Boimater.* **73** 1317
[20] Kim T H and Chang Song K 2021 *Opt. Mater.* **119** 111401
[21] Tomić S L, Jovašević J S and Filipović J M 2013 *Polym. Bull.* **70** 2895
[22] Oucif A, Haddadine N, Zakia D, Bouslah N, Benaboura A, Beyaz K, Guedouar B and El-Shall M S 2022 *Polym. Bull.* **79** 1535
[23] Liu D, Tang J, Shen L, Liu S, Zhu S, Wen S and Lin Q 2022 *Biomacromolecules* **23** 1581
[24] Hong Y, Liu D, Zou H, Jia Q, Tang S and Lin Q 2024 *Acta Biomater.* **178** 124
[25] Tai H *et al* 2009 *Biomacromolecules* **10** 2895
[26] Bozukova D, Pagnoulle C and Jérôme C 2013 *J. Cataract Refract. Surg.* **39** 1404
[27] Cabeza-Gil I, Pérez-Gracia J, Remón L and Calvo B 2021 *J. Mech. Behav. Biomed.* **114** 104165
[28] Lane S S, Burgi P, Milios G S, Orchowski M W, Vaughan M and Schwarte E 2004 *J. Cataract Refract. Surg.* **30** 2397
[29] Ballard N and Asua J M 2018 *Prog. Polym. Sci.* **79** 40
[30] Srivastava S 2009 *Des. Monomers Polym.* **12** 1
[31] Silverstein R M and Bassler G C 1962 *J. Chem. Educ.* **39** 546
[32] Coates J 2000 *Enc. Anal. Chem.* **12** 10815
[33] Pamuła E, Błażewicz M, Paluszkiewicz C and Dobrzyński P 2001 *J. Mol. Struct.* **596** 69
[34] Mejia M and Murillo E 2016 *Polimeros* **26** 254
[35] Jamshidi A, Beigi F A K, Kabiri K and Zohuriaan-Mehr M J 2005 *Polym. Test.* **24** 825
[36] Chiarcos R, Antonioli D, Sparnacci K, Gabano E, Laus M and Gianotti V 2020 *Int. J. Polym. Anal. Charact.* **25** 188
[37] Viljanen E K, Langer S, Skrifvars M and Vallittu P K 2006 *Dent. Mater.* **22** 845
[38] Codari F, Moscatelli D, Storti G and Morbidelli M 2010 *Macromol. Mater. Eng.* **295** 58
[39] Wang B, Lin Q, Shen C, Tang J, Han Y and Chen H 2014 *J. Colloid. Interface Sci.* **431** 1
[40] Wei Y, Chen Y, Liu P, Gao Q, Sun Y and Huang C 2011 *Plasma Chem. Plasma Process.* **31** 811
[41] Yakimets I, Wellner N, Smith A C, Wilson R H, Farhat I and Mitchell J 2005 *Polymer* **46** 12577
[42] Nogueira P, Ramirez C, Torres A, Abad M J, Cano J, Lopez J, Lopez-Bueno I and Barral L 2001 *J. Appl. Polym. Sci.* **80** 71–80
[43] Mredha M T I, Pathak S K, Tran V T, Cui J and Jeon I 2019 *Chem. Eng. J.* **362** 325

[44] Yin F, Tang C, Li X and Wang X 2017 *Polymers* **9** 537
[45] Zhang H, Cheng Y, Hou X, Yang B and Guo F 2018 *New J. Chem.* **42** 9151
[46] Hamdan M H M, Siregar J P, Cionita T, Jaafar J, Efriyohadi A, Junid R and Kholil A 2019 *Int. J. Adv. Manuf. Technol.* **104** 1075
[47] Randhawa K S and Patel A 2021 *Ind. Lubrication Tribol.* **73** 1146
[48] Rajeesh K R, Gnanamoorthy R and Velmurugan R 2010 *Mater. Sci. Eng.* **527** 2826
[49] Zhou C, Heath D E, Sharif A R M, Rayatpisheh S, Oh B H L, Rong X, Beuerman R and Chan-Park M B 2013 *Macromol. Biosci.* **13** 1485